Int J Appl Earth Obs Geoinformation 75 (2019) 1–14

Contents lists available at ScienceDirect

Int J Appl Earth Obs Geoinformation

journal homepage: www.elsevier.com/locate/jag

Exploring the use of vegetation indices to sense canopy nitrogen to phosphorous ratio in grasses

Yasmina Loozen[a,b,*], Derek Karssenberg[b], Steven M. de Jong[b], Shuqiong Wang[a], Jerry van Dijk[a], Martin J. Wassen[a], Karin T. Rebel[a]

[a] Copernicus Institute of Sustainable Development, Faculty of Geosciences, Utrecht University, Utrecht, The Netherlands
[b] Physiscal Geography, Faculty of Geosciences, Utrecht University, Utrecht, The Netherlands

ARTICLE INFO

Keywords:
Nutrient limitation
Canopy N:P
Holcus lanatus L.
Remote sensing
Spectroradiometer
Satellite sensors

ABSTRACT

Reduced availability of plant nutrients such as nitrogen (N) and phosphorous (P) has detrimental effects on plant growth. Plant N:P ratio, calculated as the quotient of N and P concentrations, is an ecological indicator of relative N and P limitation. Remote sensing has already been widely used to detect plant traits in foliage, particularly canopy N and P concentrations and could be used to detect canopy N:P faster and at lower cost than traditional destructive methods. Despite the potential opportunity of applying remote sensing techniques to detect canopy N:P, studies investigating canopy N:P remote detection are scarce. In this study, we examined if vegetation indices developed for canopy N or P detection can also be used for canopy N:P detection. Using in situ spectrometry, we measured the reflectance of a common grass species, Yorkshire fog (*Holcus lanatus* L.), grown under different nutrient ratios and levels. We calculated 60 VIs found in literature and compared them to optimized VIs developed specifically for this study. The VIs were calculated using both the original narrow band spectra and the spectra resampled to the band properties of six satellite sensors (MSI – Sentinel 2, OLCI – Sentinel 3, MODIS – Terra/Aqua, OLI – Landsat 8, WorldView 4 and RapidEye) to investigate the influence of bandwidths and band positions. The results showed that canopy N:P was significantly related to both existing VIs (r^2 = 0.16 - 0.48) and optimized VIs (r^2 = 0.59 – 0.72) with correlations similar to what was observed for canopy N or canopy P. Existing VIs calculated with MSI and OLI sensors bands showed higher correlation with canopy N:P compared to the other sensors while the correlation with optimized VIs was not affected by the differences in sensors' bands. This study might lead to future practical applications using in situ reflectance measurements to sense canopy N:P in grasslands.

1. Introduction

Nutrients play an essential role in plant growth and foliage nutrient concentration is linked to several physiological and ecosystem processes. Chlorophyll content, photosynthetic capacity, leaf life span, light use efficiency and biomass primary productivity have all been related to foliar nitrogen (N) concentration at the leaf or canopy level (Bakker et al., 2011; Evans, 1989; Green et al., 2003; Kergoat et al., 2008; Reich, 2012; Reich et al., 1999; Wright et al., 2004). Similarly, foliage phosphorus (P) has been correlated to leaf life span and photosynthetic capacity (Wright et al., 2004) and influences the photosynthetic rate (Vcmax) (Walker et al., 2014). Non-optimal levels of foliar N and P will often result in reduced plant growth (Zhao and Zeng, 2009).

Plant N:P ratio, defined as the quotient of plant N and plant P concentrations and expressed in g N/g P (Güsewell, 2004), is an ecological indicator of the relative N and P limitation (Koerselman and Meuleman, 1996; Olde Venterink et al., 2003; Wassen et al., 1995). Several studies have identified threshold plant N:P ratio values for N and P limitation in different ecosystems (Güsewell et al., 2003; Koerselman and Meuleman, 1996; Li et al., 2011; Olde Venterink et al., 2003; Tessier and Raynal, 2003). Although threshold values defined by different authors may vary, in general it is safe to conclude that plant N:P ratio values lower than 10 tend to indicate N limitation, while values higher than 20 are an indication of P deficiency (Güsewell, 2004). However, this ratio should be understood as a continuous gradient including a range of values (c. 10 to c. 20) in which co-limitation may occur where both N and P are in low supply (Güsewell, 2004). At

* Corresponding author at: Copernicus Institute of Sustainable Development, Princetonlaan 8a, 3584CB Utrecht, The Netherlands.
E-mail address: y.m.a.loozen@uu.nl (Y. Loozen).

https://doi.org/10.1016/j.jag.2018.08.012
Received 11 June 2018; Received in revised form 8 August 2018; Accepted 10 August 2018
Available online 23 October 2018

vegetation level, the N:P ratio is an informative variable that not only indicates potential limitation of N and P but which is also related to species composition, species richness, productivity and functional trait composition (Fujita et al., 2014; Roeling et al., 2018; Wassen et al., 2005).

Foliar N and P concentration can be measured in the laboratory, but this is labor intensive and expensive, especially for large sample sizes. An alternative approach consists of using remote sensing to estimate plant traits, among which foliage nutrient concentration (Homolová et al., 2013). Foliage N concentration influences the reflectance spectra through specific absorption features attributed to N-bonds and protein absorption. These absorption features are located at 1020 nm, 1510 nm, 1940 nm, 2060 nm, 2180 nm, 2300 nm and 2350 nm (Kumar et al., 2006). However, due to the overlapping absorption features of multiple compounds as well as the strong absorption by water in the shortwave-infrared region (SWIR, 1400 – 3000 nm), the interpretation of the reflectance spectra is difficult (Kumar et al., 2006). For this reason, foliage N detection by remote sensing is mainly linked to chlorophyll absorption and often includes regions of the spectrum associated with chlorophyll detection, i.e. the red-edge and near-infrared (NIR) regions (Schlemmer et al., 2013). Field spectrometry has been extensively applied to estimate canopy N in a variety of crops using so called spectral vegetation indices (VIs), which consist of a combination of spectral reflectance bands (Hansen and Schjoerring, 2003; Li et al., 2014; Schlemmer et al., 2013; Tian et al., 2011). Other ecosystems have been investigated for canopy N estimation using VIs computed from airborne or spaceborne sensors at different spatial resolutions, including temperate forests (HySpex airborne sensor at 3 m, Wang et al. (2016b)), tropical forests (RapidEye satellite sensor at 5 m, Cho et al. (2013)), Mediterranean forests (MERIS satellite sensor at 1 km, Loozen et al. (2018)), as well as chaparral vegetation (AVIRIS airborne sensor at 18 m, Serrano et al. (2002)) and savannah (RapidEye satellite sensor at 5 m, Ramoelo et al. (2012)).

Similar to canopy N, canopy P has been estimated using spectral indices, though to a lesser extent. Several studies have aimed to develop VIs for canopy P estimation in agricultural lands (Kawamura et al., 2011; Mahajan et al., 2014; Pimstein et al., 2011) and in a *Carex* dominated grassland (Wang et al., 2016a), all using field spectrometry.

VIs calculated from spectrometry measurements have already been extensively studied for canopy N detection (Pacheco-Labrador et al., 2014) and high accuracy results have been obtained (Tian et al., 2011). Different categories of VIs exist, the most common ones being the simple ratio (SR), the normalized difference (ND) and the simple difference (SD) (Tian et al., 2011; Wang et al., 2016a). A VI can be classified as either narrowband or broadband (Thenkabail et al., 2002). Narrowband VIs are computed from narrow reflectance bands measured through imaging spectrometry, which includes in situ reflectance measurement using a spectroradiometer as well as reflectance measured by specific airborne or spaceborne sensors (Tian et al., 2011; Wang et al., 2015). Broadband VIs are traditionally obtained from multispectral satellite sensors although they can also be computed from resampled narrow reflectance bands obtained from other sources (Clevers and Gitelson, 2013). A common approach to develop VIs is by selecting the optimal indices from all pair-wise combinations of wavelengths in the visible, NIR and shortwave-infrared (SWIR) regions (400–2500 nm), i.e. a band combination analysis (Hansen and Schjoerring, 2003; Tian et al., 2011).

Canopy N:P is relevant to ecological studies as it is a nutrient limitation indicator. It is thus somewhat surprising that remote sensing of canopy N:P using VIs has rarely been investigated. One study investigated canopy N:P detection in savanna grasslands using field spectrometry coupled with partial least square regression with significant results (r^2 = 0.69 – 0.85, Ramoelo et al., 2013). Canopy N:P detection was also investigated in a boreal forest using vegetation indices calculated from airborne (Compact Airborne Spectrographic Imager, CASI) and spaceborne (Hyperion EO-1) imaging spectrometry (Gökkaya et al., 2015). The results showed that the VIs could be related to canopy N:P with r^2 ranging from 0.34 to 0.70. In this context, there is a need to examine in more detail how spectral properties, either from in situ measurement or satellite sensors, influence the performance of VIs regarding canopy N:P detection.

In this study, we aim at identifying if existing VIs that have been used for the estimation of canopy N or canopy P can also be used to remotely sense canopy N:P. To do so, we will evaluate three sub questions. How do VIs perform for canopy N:P estimation compared to canopy N and canopy P estimation? How do existing VIs perform compared to optimized VIs developed using the data collected in this study? How is the correlation between canopy N:P and the VIs influenced by different sensors' bandwidths and band positions?

To create a data set representing a large range of canopy N:P values, we chose to execute the study under controlled conditions. We have grown a common temperate grassland species, *Holcus lanatus* L. using six nutrient treatments that reflect N limited, P limited, and N and P co-limited conditions, under high and low nutrient availability, respectively. Existing VIs found in the literature were computed using the original narrow band reflectance spectra measured by in situ spectrometry as well as the resampled spectra corresponding to six different satellites sensors (MSI aboard Sentinel 2, OLCI aboard Sentinel 3, MODIS aboard Terra-Aqua, OLI aboard Landsat 8, WorldView 4 and RapidEye). We compared the existing VIs to optimized VIs, obtained using a band combination analysis carried out on both the original narrow band spectra and the resampled broadband spectra.

2. Material and methods

2.1. Culture of the plants

Holcus lanatus L. (Yorkshire fog) is a perennial common grass species, generally found on nutrient-rich soils throughout Europe. Seeds were collected from the Middenduin nature reserve (52 °24′N 4 °35′E) located in the western Netherlands and cultivated under controlled conditions in a greenhouse of Utrecht University. Seeds were sown on moist quartz sand and were transplanted after 22 days into pots containing a mixture of quartz sand (Carlo Bernasconi, Zürich, CH, 0.1–0.7 mm) and sand collected close to the area where seed were harvested under a ratio of 11:1. This was done to introduce soil fauna, bacteria and fungi for a complete soil community. Each pot was planted with four seedlings. Plants were grown further under nutrient treatments that lasted from July 2015 until June 2016 in the greenhouse with 400 Wm^{-2} light from 9:00 am to 4:00 pm and a temperature regime that mimicked the temperate conditions of the Netherlands. Six nutrient treatments were applied with three N:P ratios, each in high and low nutrient supply levels. The nutrient ratios were N:P = 5 (N-limitation), N:P = 15 (balanced supply) and N:P = 45 (P-limitation). Each nutrient treatment had 8 replicates (n = 48). The nutrient treatments were applied following Güsewell (2005). N was supplied as KNO_3 and $Ca(NO_3)_2$, P was provided as KH_2PO_4. KNO_3 and KH_2PO_4 supplied part of the potassium, the rest was added as KCl. All the other essential macro- and micro-nutrients were provided in non-limiting supply using a standard Hoagland solution.

2.2. Reflectance measurements

The canopy reflectance of the grasses was measured inside the greenhouse under controlled conditions when plants were fully grown on February 19th 2016 using a FieldSpec Pro Fr spectroradiometer (Analytical Spectral Device, Boulder, GO, USA). This device measures reflectance between 350 and 2500 nm with a resampled spectral resolution of 1 nm. We performed the spectral measurements with several lamps positioned above the plants on each side of the spectroradiometer to ensure constant light conditions. The spectroradiometer was held by a tripod at nadir position approximately 20 cm above the canopy. The field of view was 8°, ensuring a ground field of view of approximately 12 cm^2. Each measurement of the spectroradiometer was the average of 50 successive scans. We measured each pot four times, after turning the pot by 90 degrees between each measurement to reduce geometrical effects. We averaged these four measurements to produce one canopy measurement per pot. The spectroradiometer was internally calibrated using a Spectralon white reference panel (Labsphere, North Sutton, NH, USA).

2.3. Leaf chemical measurements

Two leaves were sampled from each pot (n = 48) on February 25th 2016, collected in paper bags and dried in an oven at 60 °C for 48 h. The leaf samples were then ground using mixer mill (MM400, Retsch). The N concentration (g N 100 g^{-1} dry matter, %N) was measured using an elemental CN analyzer (Fisons NA 1500 NCS). The P concentration (g P 100 g^{-1} dry matter, %P) was measured using the total reflection X-ray fluorescence spectroscopy method (TXRF, S2 Picofox, Bruker, Germany). N:P ratios were calculated as the ratio between the weight based concentrations of N and P.

2.4. Spectral bands considered: original and resampled to satellite bands

Prior to analysis, the spectral range was reduced from 350–2500 nm to 400–2450 nm because the signal to noise ratio was too low for the minimum and maximum spectral ranges. This spectral range matches with the spectral coverage of earth observation sensors. We considered two sets of spectral bands: the original narrow band reflectance spectra and the spectra resampled to the properties of satellite sensor bands. We included the spectra resampled to satellite sensor bands to assess the possibility of detecting canopy N:P with VIs derived from actual satellite measurements. We included six different satellite sensors (MSI-Sentinel-2, OLCI-Sentinel-3, MODIS-Terra/Aqua, OLI-Landsat 8, WorldView 4, and RapidEye). We chose these sensors because they present a variety of band properties, from 5 to 21 bands and from 2.5 nm to 350 nm spectral resolution (Table 1, Fig. 1). They are all operational and have a long measurement record in the case of MODIS and Landsat. We obtained the resampled spectra by using the spectral response function corresponding to each sensor band. The spectral response functions were downloaded from the website of the sensor producer. For the MODIS sensor, the measured spectral response function could not be found and was approximated using a standard normal distribution (μ = 0, σ = 1).

2.5. Data analysis

2.5.1. Descriptive statistics and vegetation indices

Descriptive statistics and boxplots of canopy N:P, N and P, hereafter designated as canopy traits, were produced and the Pearson correlation coefficients between each of these canopy traits were calculated.

2.5.2. Existing VIs

We evaluated existing VIs, which we selected through a literature search. We found 60 VIs to evaluate (Table A1), including VIs that were either developed for N or P detection or, when developed for another purpose, for instance VIs correlated with chlorophyll, photosynthesis or the presence of vegetation (see the "developed for" column of the Table A1 for a detailed list), have been used for N or P detection.

Based on their equations, we categorized the VIs as either two bands simple ratio (SR, $\frac{band_1}{band_2}$), two bands normalized difference (ND, $\frac{band_1 - band_2}{band_1 + band_2}$) or three bands VI (TB). When they did not belong to any of the aforementioned categories, they were labelled other VI (OVI, see Table A1 for equations associated with TB or OVI).

We calculated linear models between canopy N:P, canopy N or canopy P and both the VIs and the natural log transformed VIs calculated using the original narrow band spectra.

The ten narrow band VIs that obtained the best correlation (r^2) with canopy N:P were also calculated using the spectra resampled to the six satellite sensor bands mentioned in section 2.4. The indices were computed using the sensor bands closest to the VI nominal wavelengths. Several VIs could not be computed because the sensors' band locations were too distant (> 100 nm) from the VI nominal wavelength.

2.5.3. Optimized VIs

From the spectral signature we took from our experimental data, we calculated optimal VIs using combinations of all available wavelengths, i.e. a band combination analysis. Following Tian et al. (2011), every combination of two, λ_1 and λ_2, or three wavelengths, λ_1, λ_2 and λ_3, was used to compute two bands or three bands VIs. The two bands VIs were categorized as simple ratio (SR) $\frac{\lambda_1}{\lambda_2}$, single difference (SD) $\lambda_1 - \lambda_2$ and normalized difference (ND) $\frac{|\lambda_1 - \lambda_2|}{\lambda_1 + \lambda_2}$, while the three bands indices were named TB1 $\frac{\lambda_1}{\lambda_2 + \lambda_3}$, TB2 $\frac{\lambda_1 - \lambda_2}{\lambda_1 + \lambda_3}$ and TB3 $\frac{\lambda_1 - \lambda_2 + 2*\lambda_3}{\lambda_1 + \lambda_2 - 2*\lambda_3}$. In order to decrease computation time, the three bands VIs were computed using only 1 out of 10 narrow bands (Pacheco-Labrador et al., 2014). Subsequently, linear regressions between each of the obtained VIs and canopy N:P, canopy N and canopy P were calculated. Specific wavelength regions of high correlation between the canopy traits and the three categories of two bands VI were identified using heatmaps. The optimized VIs were

Table 1
Properties of the six satellite sensors included in this study.

Satellite	Sensor	Number of bands	Bandwidth (nm)	Spatial resolution (m)
Sentinel 2	MSI	13	15 - 180	10 - 20 - 60
Sentinel 3	OLCI	21	2.5 - 40	300 - 1200
Terra - Aqua	MODIS	20	10 - 50	250 - 500 -1000
Landsat 8	OLI	9	20 - 200	30
WorldView 4	WorldView 4	5	35 - 350	0.31 - 1.24
RapidEye	RapidEye	5	40 - 70	5

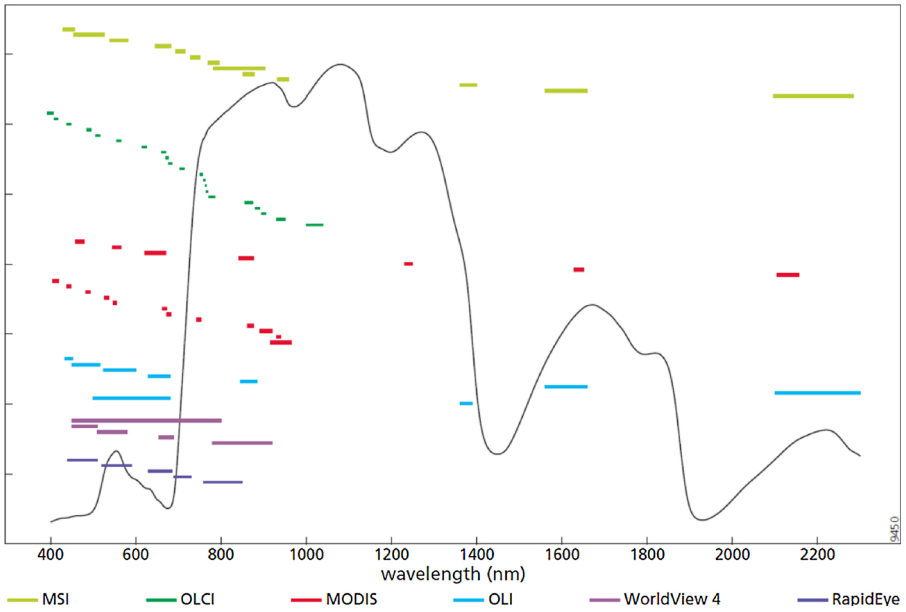

Fig. 1. Spectral band position and bandwidth of the six satellite sensors included in the analysis (MSI, OLCI, MODIS, WorldView 4; RapidEye) projected on a Yorkshire fog (Holcus lanatus) reflectance spectrum measured using a spectroradiometer.

obtained by selecting the band combination with the highest r^2, for both the narrow band spectra and the spectra resampled to satellite sensor bands.

2.5.4. Regression models

All regression models were assessed using the determination coefficient (r^2) and the cross validated Relative Root Mean Square Error ($RRMSE_{cv}$) values, obtained using the leave-one-out cross validation method (Clevers and Gitelson, 2013) and calculated following Eq. (1) (Yao et al., 2010):

Table 2
Pearson correlation matrix between canopy N, canopy P and canopy N:P. The values in the lower part of the table correspond to the correlation coefficients while the upper part of the table corresponds to the p-values.

	canopy N	canopy P	canopy N:P
canopy N	/	*p-value* = 0.000	*p-value* = 0.000
canopy P	r = -0.66	/	*p-value* = 0.000
canopy N:P	r = 0.92	r = -0.81	/

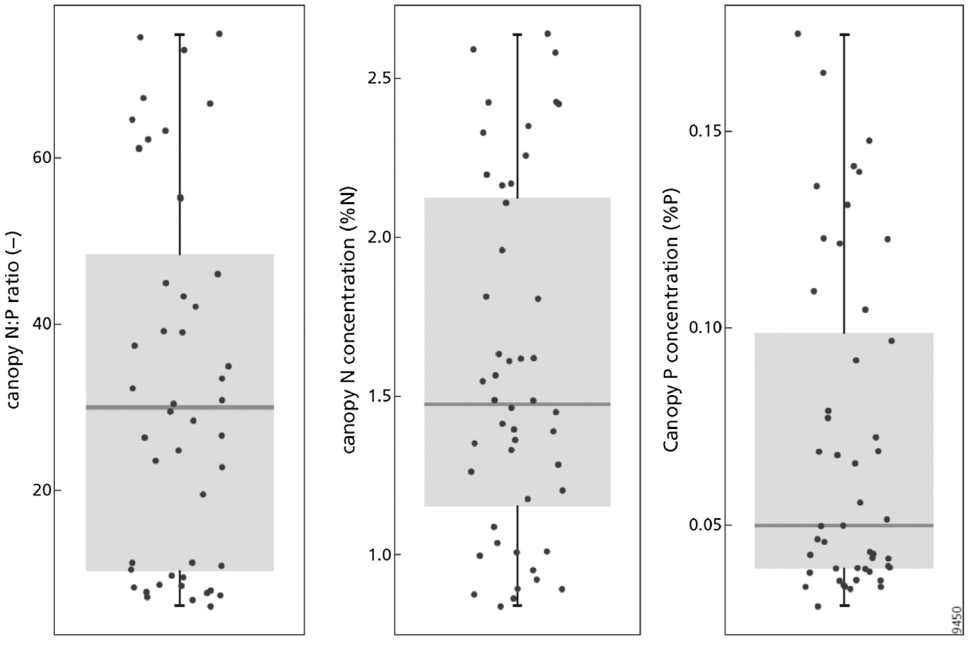

Fig. 2. Boxplot of canopy N:P (-), canopy N (%N) and canopy P (%P) in Holcus lanatus L. grasses (n = 48).

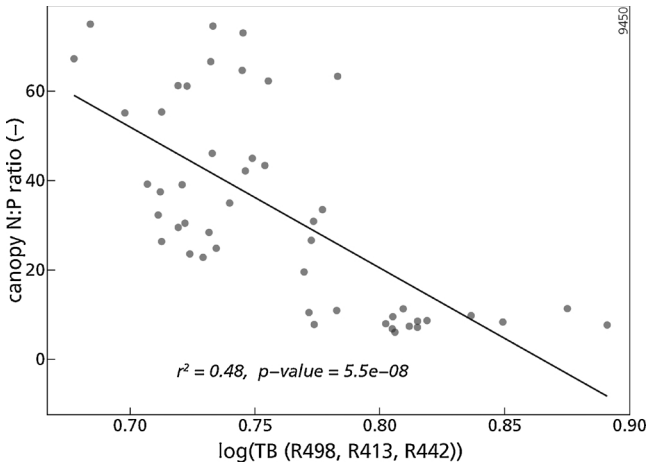

Fig. 3. Scatterplot and regression line between canopy N:P and the TB (R_{498}, R_{413}, R_{442}) vegetation index, i.e. the existing vegetation index with the highest correlation with canopy N:P (r^2 = 0.48, n = 48). The vegetation index was calculated using the original narrow band spectra.

$$RRMSEcv = \sqrt{\frac{1}{n} \times \sum_{i=1}^{n} (P_i - O_i)^2} \times \frac{1}{\bar{O}_i} \quad (1)$$

where $i = 1, 2, ..., n$ is a measurement, with n the total number of measurements, P_i represents the predicted value, O_i, the observed value, and $\bar{O}_i$ the mean of all observed values. The significance level was at a *p-value* < 0.01. All the statistical analyses were performed in the R environment (R Development Core Team, 2014).

3. Results

3.1. Descriptive statistics of canopy N:P, canopy N and canopy P

The results of the descriptive statistics showed that the range of canopy N:P values (6.1–75.0, Fig. 2) corresponds to the range usually observed in natural environments (Roeling et al., 2018). As expected, canopy N:P was correlated with both canopy N and canopy P (Table 2).

3.2. Original narrow band spectra

3.2.1. Existing vegetation indices

Among the 60 existing VIs tested, 31 VIs showed significant relationships with at least one canopy trait, while 29 VIs showed no significant relationship with any of the canopy traits (Table A1). The VI showing the highest correlation with canopy N:P (r^2 = 0.48), was the TB (R_{498}, R_{413}, R_{442}, Fig. 3) VI developed for N detection (Tian et al., 2011). The results obtained for canopy N and canopy P were similar, with the highest r^2 equal to 0.44 for canopy N with ND (R_{1220}, R_{710}) VI. For canopy P, the highest correlation (r^2 = 0.52) was obtained with TB (R_{498}, R_{413}, R_{442}), hence the same VI as for canopy N:P. The two VIs showing the highest correlation with canopy N:P, TB (R_{498}, R_{413}, R_{442}) and TB (R_{434}, R_{496}, R_{401}) were both based on three wavelengths located in the blue region of the spectrum. Other VIs that showed a significant

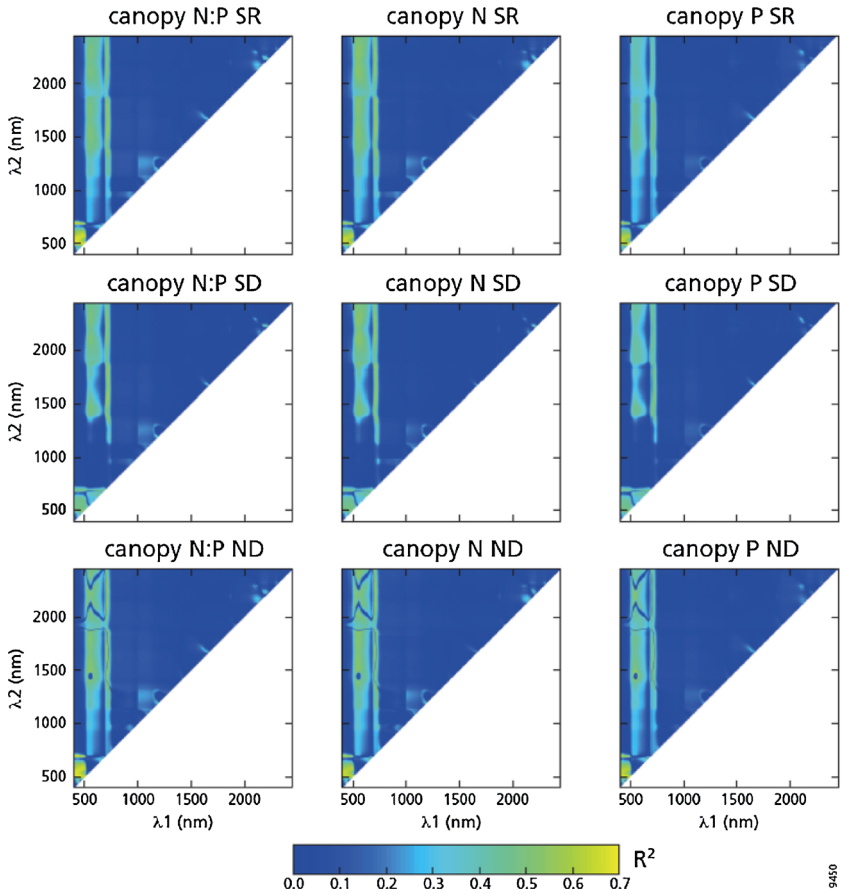

Fig. 4. Heatmaps showing the coefficient of determination (r2) between the canopy trait and each combination of two bands (λ1 and λ2, nm) between 400–2450 nm for canopy N:P, canopy N and canopy P and each VI category investigated. SR, Simple Ratio; SD, Simple Difference, ND, Normalized Difference.

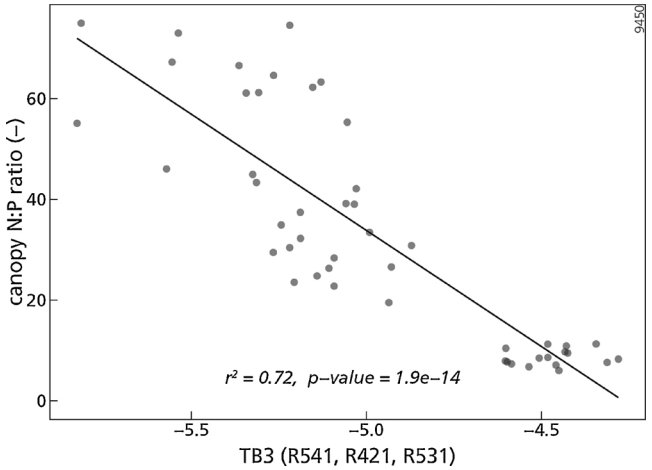

Fig. 5. Scatterplot and regression line between canopy N:P and the TB3 (R_{541}, R_{421}, R_{531}) vegetation index, i.e. the optimized vegetation index with the highest correlation with canopy N:P (r^2 = 0.72, n = 48). The vegetation index was calculated using the original narrow band spectra.

relationship with canopy N:P were based on the NIR and red-edge regions of the spectrum.

3.2.2. Optimized vegetation indices

We used heatmaps to investigate the wavelength regions of high correlation between the two bands VIs, obtained from the band combination analysis, and the three canopy traits (Fig. 4). A first region of high correlation with canopy N:P (r^2 between 0.4 and 0.7) was located in the blue region for λ_1 (400–500 nm) and in the green – red region for λ_2 (500–700 nm). A second region (r^2 between 0.4 and 0.6) was located in the green – red region for λ_1 (500–700 nm) and in the SWIR region for λ_2 (1400–2450 nm). The regions of high correlation with canopy N:P were similar across the VIs categories investigated, i.e. SR, SD and ND, and also had high correlations for canopy N and canopy P.

The optimized VI TB3 (R_{541}, R_{421}, R_{531}, Fig. 5), located in the blue and green region of the spectrum showed the highest correlation with canopy N:P and had a higher r^2 (r^2 = 0.72, Table A2) than the best performing optimized VIs for canopy N (r^2 = 0.69; TB3, R_{431}, R_{2431}, R_{561}) and for canopy P (r^2 = 0.67; TB1, R_{531}, R_{541}, R_{421}).

Regarding the influence of the VI category on the result, the optimized VIs from the SD category, which were composed of a combination of bands from the red-edge and SWIR regions, showed lower correlations (r^2 = 0.53 - 0.59) than all the other VI categories (r^2 = 0.64 – 0.72), mostly composed of a combination of blue and green bands. This result holds for all canopy traits (canopy N:P, N and P).

Compared to the results obtained for the existing VIs, the optimized VIs performed better regarding r^2 values (Fig. 6) for canopy N:P. The best optimized VI explained 24 percent more of the variation in canopy N:P values compared to the best performing existing VI.

3.3. Spectra resampled to satellite sensors' bands

3.3.1. Existing vegetation indices

The TB (R_{434}, R_{496}, R_{401}) VI calculated for the MSI sensor aboard Sentinel 2 showed the highest correlation with canopy N:P (r^2 = 0.63), canopy N (r^2 = 0.58) and canopy P (r^2 = 0.62) compared to the other existing VIs tested (Table A3). Regarding the influence of the sensor band properties on the result, the existing VIs calculated using the MSI and OLI sensors band showed in general higher correlation with canopy N:P than the same VIs calculated based on OLCI or MODIS sensors (Fig. 7). For the existing VIs TB (R_{498}, R_{413}, R_{442}), TB (R_{434}, R_{496}, R_{401}) and TB (R_{705}, R_{717}, R_{491}) calculated based on MSI sensor bands, the TB (R_{498}, R_{413}, R_{442}) and TB (R_{434}, R_{496}, R_{401}) VIs calculated based on OLI sensor bands as well as for the TB (R_{705}, R_{717}, R_{491}) VI calculated based on OLCI sensor properties, the obtained r^2 were higher than for the same VIs calculated with the original narrow band spectra. Similar results were observed for canopy N and canopy P. On the contrary, all the existing VIs calculated with the spectra resampled to MODIS bands showed lower r^2 with canopy N:P compared to their narrow band

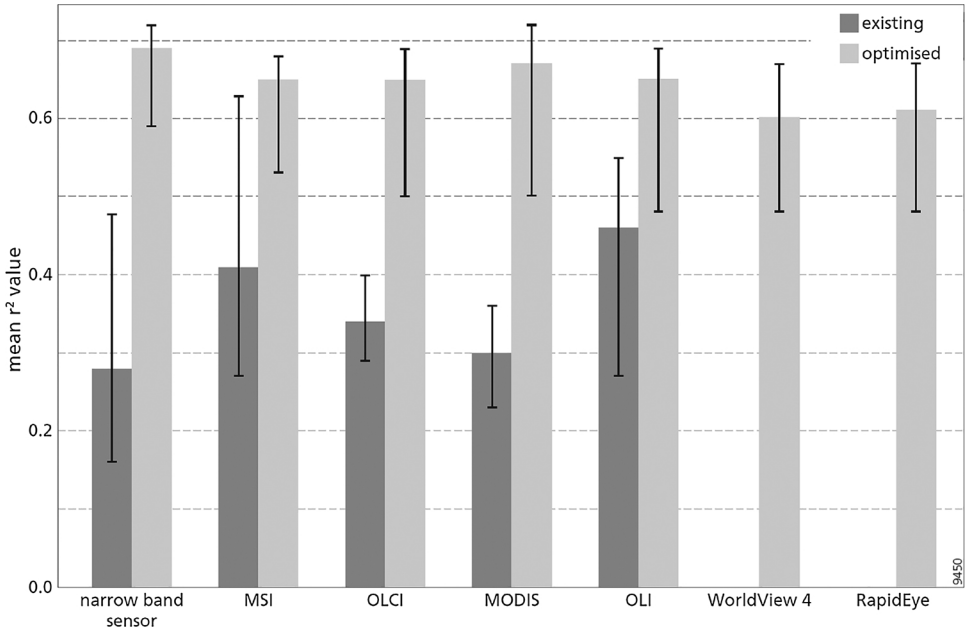

Fig. 6. Mean r^2 value of the relationship between canopy N:P and the vegetation indices (VIs) for the seven sensors included in this analysis and for both the existing and optimized VIs. The vertical lines represent the minimum and maximum r^2 obtained for each group. No existing VI was calculated for the WorldView 4 and RapidEye sensors because their band positions are too distant (> 100 nm) from the nominal VIs' wavelengths.

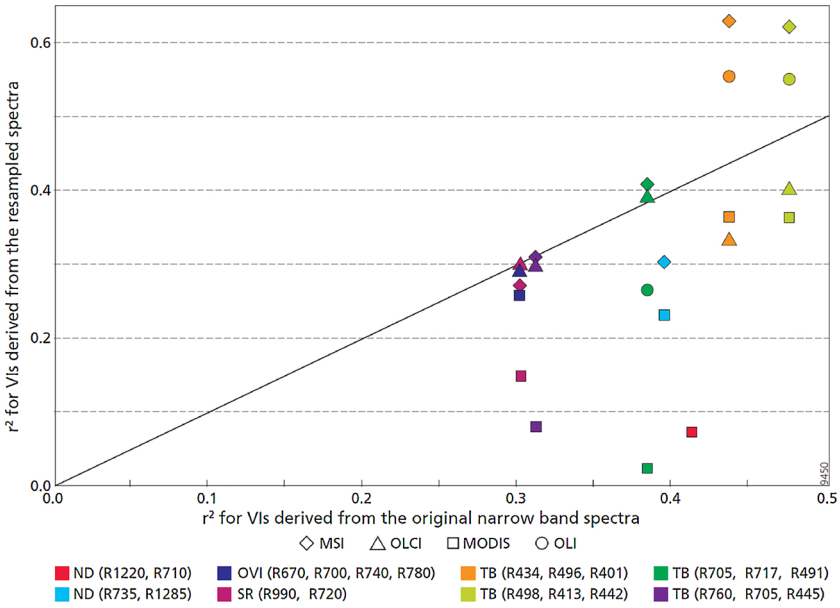

Fig. 7. Comparison between the r^2 obtained for the relationships between canopy N:P and the existing VIs calculated using either the original narrow band spectra or the spectra resample to satellite sensors'band properties (MSI, OLCI, MODIS, OLI). No existing VI was calculated for the RapidEye and WorldView 4 sensors because their band positions are too distant (> 100 nm) from the nominal VIs' wavelengths.

spectra counterpart and three existing VIs showed an non-significant relationship with canopy N:P.

3.3.2. Optimized vegetation indices

Canopy N:P could be related to the optimized VIs calculated from the resampled spectra with r^2 values ranging from 0.48 to 0.72 (Table A2). Similar results were obtained for canopy N and canopy P. The SR, ND and TB categories of optimized VIs mostly performed better with canopy N:P (r^2 between 0.55 – 0.72) compared to the SD category of VI (r^2 between 0.48 - 0.59). Among the bands selected for the SR, ND and TB categories of optimized VIs, the blue and green regions of the spectrum were dominant, similar to what was observed for narrow bands optimized VIs.

The difference in satellite sensors band properties did not greatly affect the results as the r^2 values were in the same range for all sensors per VI category. The satellite sensors WorldView 4 and RapidEye, both with five bands and bandwidths between 35–140 nm, showed r^2 between 0.55 and 0.67 with canopy N:P for the SR, ND and TB categories of VI. This is comparable to the results obtained for satellites sensors with a higher number of bands and narrower bands, e.g. MSI and MODIS, for which the obtained r^2 values were between 0.67 and 0.72 for the same VI categories.

When comparing the performance of existing and optimized VIs for canopy N:P detection (Fig. 6), optimized VIs generally performed better than existing VIs for all satellite sensors tested. However, the existing VIs calculated for the MSI and OLI sensors showed r^2 values in an overlapping range with their optimized counterparts.

4. Discussion

4.1. Original narrow band spectra

4.1.1. Existing vegetation indices

Existing VIs performed similarly for canopy N:P detection as they did for canopy N and canopy P regarding obtained r^2 values. More specifically, the two best performing VIs for canopy N:P in this study, TB (R_{498}, R_{413}, R_{442}) and TB (R_{434}, R_{496}, R_{401}), both based on the blue region of the spectrum, proved to be interesting candidates for canopy N:P detection. In previous studies, these VIs were highly correlated to canopy N in rice crops (r^2 = 0.81 and r^2 = 0.84, respectively (Tian et al., 2011), but showed a weak correlation with canopy N in Holm oak leaves (Pacheco-Labrador et al., 2014).

Among the 60 VIs tested, almost 50% (n = 29) failed to show a significant relationship with canopy N:P, canopy N or canopy P while previous studies found a significant relationship. This unreliability in prediction accuracy for previously validated VIs was already observed by Pacheco-Labrador et al. (2014), who found that the majority of the published vegetation indices tested could not be correlated to canopy N in Holm oak leaves. This might be explained by differences in growth conditions and species investigated as well as by the influence of the range in canopy N or canopy P values. This highlights the influence of the dataset on the prediction accuracy.

4.1.2. Optimized vegetation indices

The optimized VIs developed specifically for this study performed better for canopy N:P detection compared to the existing VIs tested, for both r^2 and $RRMSE_{cv}$ values.

The SR, ND and TB categories of optimized VIs were based on a combination of wavelengths from the blue and green regions of the spectrum. The blue region is linked to pigment absorption, which peaks at 430 nm for chlorophyll *a* (chlor-a) and 460 nm for chlorophyll b (chlor-b) (Kumar et al., 2006). The SD, ND and TB_3 optimized VIs for canopy N:P included wavelengths located at 427 nm and 421 nm, hence close to one of the absorption peaks of chlor-a. Other indices located in the blue and green regions of the spectrum have been related to chlor-a and chlor-b concentration in *Vitis vinifera* leaves (the BGI2 index, SR, R_{450}, R_{550}; Zarco-Tejada et al. (2005)) or to canopy N in rice (ND, R_{573}, R_{444}; Tian et al. (2011)). The combination of wavelengths from the blue and green regions might thus be linked with chlorophyll and has also been explored for canopy N detection (Tian et al., 2011). Our results

showed that this wavelength combination is correlated with canopy N:P, canopy N and canopy P.

The optimized SD VI for canopy N:P combined wavelengths located in the red-edge (718 nm) and in the SWIR regions (1577 nm). The SWIR region is characterized by several nitrogen and protein absorption features. The absorption features located at 1500 nm and 1510 nm might explain the second wavelength (1577 nm) being selected, because the absorption features are known to be broadened due to scattering (Kumar et al., 2006). However, the SWIR region of the spectra is influenced by the absorption features of many compounds that interfere with each other (Kumar et al., 2006) which render the signal difficult to interpret. In particular, the strong absorption due to water molecules greatly influences the reflectance. This might be the reason why the proportion of variance explained by the SD category of optimized VIs (r^2 = 0.53 – 0.59) was lower than for the SR, ND and TB categories of optimized VIs (r^2 = 0.64 – 0.72).

4.2. Spectra resampled to satellite sensors' bands

4.2.1. Existing vegetation indices

The correlation between canopy N:P and the existing VIs was influenced by the sensors' band properties because different sensors showed different correlation with canopy N:P for the same VIs. Two VIs (TB R_{498}, R_{413}, R_{442} and TB R_{434}, R_{496}, R_{401}) calculated from MSI and OLI sensors showed higher correlation (r^2 = 0.55 – 0.63) than when calculated from the OLCI and MODIS sensors (r^2 = 0.36 – 0.40) or even narrow band sensors (r^2 = 0.44 – 0.48) (Fig. 7). The bands from MSI and OLI sensors used for the VIs calculation were broader than their counterparts from the OLCI and MODIS sensors and hence from the original narrow band spectra. The bandwidth of the sensors thus influenced the correlation obtained for some of the existing VIs.

4.2.2. Optimized vegetation indices

The correlation between canopy N:P and the optimized VIs was not greatly influenced by the sensors' band properties and the correlation was stable across the different satellite sensors tested. Although this is in contradiction to what was observed for existing VIs, this might indicate that broad band sensors, such as RapidEye and WorldView 4, could be useful for canopy N:P detection. However, our results consistently showed that the blue region was important for canopy N:P detection. Although VIs based on the blue region of the spectrum do not represent a difficulty for in situ studies, including the blue region for VIs calculated from satellite sensors might lead to an interpretation problem due to atmosphere Rayleygh scattering.

4.3. Future perspectives

This analysis investigated the possibility of detecting canopy N:P using VIs compared to canopy N and canopy P detection as well as the influence of the sensors band properties on the relationships. The results obtained in this analysis might have concrete in-situ application perspectives in the field of ecology given the importance of the canopy N:P for biodiversity studies (Fujita et al., 2014; Roeling et al., 2018; Wassen et al., 2005). Spectral VIs might be a useful method to detect canopy N:P in grasslands in a non-destructive and time efficient manner that would, for example, allow to monitor the seasonal evolution of canopy N:P or trends in changing N:P ratios in response to eutrophication or other global change factors (Wassen et al., 2013). However, as with remote sensing of canopy N or canopy P, remote sensing of canopy N:P is not a direct measurement of canopy N:P values. Especially, the correlation between canopy N:P and both canopy N and canopy P (Table 2) renders it difficult to distinguish between the separate influences on the reflectance signal. Moreover, similar studies investigating canopy N:P detection should be done on more plant species and plant communities in order to validate the results obtained in this study. Further studies should also investigate the influence of the spatial resolution of the satellite sensors on canopy N:P detection as this needs to be studied before actual satellite sensors measurements can be exploited to sense canopy N:P in natural environment.

5. Conclusion

Canopy N remote detection has already been extensively studied using both spectroradiometer and satellite measurements. On the contrary, canopy N:P, despite being an important indicator of nutrient limitation, has seldom been studied with remote sensing techniques. In this study, we investigated the possibility of detecting canopy N:P in the common grass species *Holcus lanatus* using VIs developed for canopy N and canopy P detection. The results showed that using VIs for canopy N:P detection was as effective as when applied for canopy N or canopy P detection. This held for both existing and optimized VIs as well as for narrow band and broader band VIs calculated from the spectra resampled to the spectral properties of six different satellite sensors. The influence of different satellite sensors' band properties was unclear as it differed between existing and optimized VIs. Existing VIs calculated with MSI and OLI sensors bands showed higher correlation with canopy N:P compared to the other sensors tested. In contrast, the correlation with optimized VIs was not affected by the differences in sensors' bands. Satellite sensors with a limited number of broad bands, such as WorldView 4 and RapidEye, yielded similar results as sensors with multiple and narrower bands, like MSI or Sentinel 3. In the future, these results might lead to practical applications using handheld spectrometers for in situ canopy N:P detection in grasslands. The observed consistent importance of the blue region of the spectrum for canopy N:P detection might render canopy N:P detection with actual satellite sensors complicated due to the interference with the Rayleygh scattering.

Competing interest

The authors declare that they have no competing interests.

Acknowledgments

This work was supported by The Netherlands Organization for Scientific Research (NWO) [NWO ALW-GO-AO/14-12]. We would like to acknowledge Ton Markus for his help with the figures presented in this paper.

Appendix A

Table A1
Relationship between the existing vegetation indices (VIs) (n = 60) and canopy N:P, canopy N and canopy P. Coefficient of determination (r^2), p-value and Relative Root Mean Square Error of cross-validation (RRMSEcv). For each VI, the best model, linear (L) or logarithmic (LOG), based on r^2 value, is presented. The VIs were classified into four categories: ND = normalized difference; SR = simple ratio; TB = three band; OVI = other vegetation index. The VIs are sorted from the highest to the lowest correlation with canopy N:P.

VI	Canopy N:P				*Canopy N*				Canopy P				Equation	Developped for	References
	Model	r^2	*p-value*	RRMSEcv	*Model*	*r^2*	*p-value*	*RRMSEcv*	Model	r^2	*p-value*	RRMSEcv			
TBVI (R498, R413, R442)	LOG	0.48	0.000	0.50	*LOG*	*0.42*	*0.000*	*0.27*	LOG	0.52	0.000	0.43	(R498 + R413)/R442	N detection	(Tian et al., 2011)
TBVI (R434, R496, R401)	L	0.44	0.000	0.52	*L*	*0.38*	*0.000*	*0.28*	LOG	0.48	0.000	0.44	R434/(R496 + R401)	N detection	(Tian et al., 2011)
NDVI (R1220, R710)	L	0.41	0.000	0.54	*LOG*	*0.44*	*0.000*	*0.26*	LOG	0.37	0.000	0.48	(R1220 − R710)/(R1220 + R710)	N detection	(Zhu et al., 2007a)
NDVI (R693, R1770)	L	0.40	0.000	0.54	*L*	*0.39*	*0.000*	*0.28*	L	0.34	0.000	0.49	(R693 - R1770) / (R693 + R1770)	N detection	(Ferwerda et al., 2005)
NDVI (R735, R1285)	L	0.40	0.000	0.54	*L*	*0.44*	*0.000*	*0.27*	L	0.30	0.000	0.50	(R735 -R1285) / (R735 + R1285)	N detection	(Pacheco-Labrador et al., 2014)
TBVI (R705, R717, R491)	L	0.38	0.000	0.55	*L*	*0.37*	*0.000*	*0.28*	L	0.36	0.000	0.48	R705/(R717 + R491)	N detection	(Tian et al., 2011)
TBVI (R760, R705, R445)	L	0.31	0.000	0.58	*LOG*	*0.32*	*0.000*	*0.29*	LOG	0.32	0.000	0.49	(R760 - R705)/(R760 + R705 - 2*R445)	N detection	(Tian et al., 2011)
TBVI (R760, R723, R2387)	LOG	0.31	0.000	0.58	*LOG*	*0.34*	*0.000*	*0.29*	LOG	0.30	0.000	0.50	(R760 - R2387)/(R723 - R2387)	P detection	(Wang et al., 2016a)
SR (R990, R720)	LOG	0.30	0.000	0.59	*LOG*	*0.35*	*0.000*	*0.28*	LOG	0.28	0.000	0.51	R 990 / R720	N detection	(Yao et al., 2010)
OVI (R670, R700, R740, R780) REP	LOG	0.30	0.000	0.58	*LOG*	*0.33*	*0.000*	*0.29*	LOG	0.33	0.000	0.49	700 + 40 * (((R670 + R780)/2 - R700) / (R740 -R700))	red-edge	(Horler et al., 1983)
TBVI (R924, R703, R423)	LOG	0.30	0.000	0.58	*LOG*	*0.32*	*0.000*	*0.29*	LOG	0.30	0.000	0.50	(R924 - R703 + 2*R423) / (R924 + R703 + 2*R423)	N detection	(Wang et al., 2012)
SR (R1220, R610)	LOG	0.30	0.000	0.58	*LOG*	*0.31*	*0.000*	*0.29*	LOG	0.26	0.000	0.52	R1220 / R610	N detection	(Zhu et al., 2007b)
TBVI (R754, R709, R681) MTCI	LOG	0.29	0.000	0.59	*LOG*	*0.31*	*0.000*	*0.29*	LOG	0.31	0.000	0.50	(R754 − R709)/(R709 − R681)	red-edge - chlorophyll	(Dash and Curran, 2004)
SR (R550, R800)	L	0.27	0.000	0.59	*L*	*0.30*	*0.000*	*0.29*	L	0.29	0.000	0.51	R550 / R 800	chlorophyll	(Buschmann and Nagel, 1993)
TBVI (R1310, R1720, R730)	LOG	0.27	0.000	0.60	*LOG*	*0.33*	*0.000*	*0.29*	LOG	0.22	0.001	0.53	R1310/(R1720 + R730)	N detection	(Pacheco-Labrador et al., 2014)
NDVI (R850, R550) Green NDVI	LOG	0.27	0.000	0.59	*LOG*	*0.30*	*0.000*	*0.29*	LOG	0.28	0.000	0.51	(R850 - R550) / (R850 + R550)	chlorophyll	(Gitelson et al., 1996)
OVI (R790, R550) Clgreen	LOG	0.27	0.000	0.60	*LOG*	*0.30*	*0.000*	*0.30*	LOG	0.28	0.000	0.51	R790/R550 − 1	red-edge - chlorophyll	(Gitelson et al., 2005)
TBVI (R720, R860, R450)	L	0.26	0.000	0.60	*L*	*0.29*	*0.000*	*0.30*	L	0.27	0.000	0.51	(R720 - R450)/(R860 - R450)	chlorophyll	(le Maire et al., 2008)
SR (R810, R560)	LOG	0.25	0.000	0.60	*LOG*	*0.28*	*0.000*	*0.30*	LOG	0.26	0.000	0.52	R 810 / R560	N detection	(Xue et al., 2004)
NDVI (R750, R705)	L	0.24	0.000	0.61	*LOG*	*0.25*	*0.000*	*0.31*	LOG	0.26	0.000	0.52	(R750 - 705)/(R750 + 705)	N detection	(Corp et al., 2010)
NDVI (R790, R720) NDRE	LOG	0.24	0.000	0.61	*LOG*	*0.27*	*0.000*	*0.30*	LOG	0.27	0.000	0.51	(R790 − R720)/(R790 + R720)	red-edge	(Fitzgerald et al., 2010)
OVI (R790, R720) Clred-edge	LOG	0.24	0.000	0.61	*LOG*	*0.26*	*0.000*	*0.30*	LOG	0.26	0.000	0.52	(R790/R720) - 1	red-edge - chlorophyll	(Gitelson et al., 2005)
NDVI (R860, R720)	LOG	0.23	0.001	0.61	*LOG*	*0.27*	*0.000*	*0.30*	LOG	0.25	0.000	0.52	(R860 - R720)/(R860 + R720)	N detection	(Yao et al., 2010)
TBVI (R760, R734, R834)	LOG	0.22	0.001	0.62	*LOG*	*0.22*	*0.001*	*0.31*	LOG	0.20	0.001	0.54	R760/(R734 + R834)	N detection	(Tian et al., 2011)
TBVI (R715, R860, R445)	L	0.20	0.001	0.63	*L*	*0.23*	*0.001*	*0.31*	L	0.21	0.001	0.54	(R715 - 860)/(R715 + R860 + 2*R445)	chlorophyll	(le Maire et al., 2008)
TBVI (R750, R705, R445)	L	0.20	0.002	0.63	*L*	*0.21*	*0.001*	*0.32*	LOG	0.21	0.001	0.53	(R750 - 705)/(R750 + R705 + 2*R445)	chlorophyll	(Sims and Gamon, 2002)
TBVI (R708, R710, R680)	L	0.17	0.003	0.64	*L*	*0.16*	*0.005*	*0.33*	L	0.15	0.007	0.55	(R708 - R710)/(R708 - R680)	N detection	(Tian et al., 2011)
TBVI (R730, R720, R725)	L	0.17	0.004	0.64	*L*	*0.21*	*0.001*	*0.32*	L	0.20	0.002	0.54	(R730 - R725)/(R720-R725)	P detection	(Wang et al., 2016a)
TBVI (R720, R729, R726)	LOG	0.17	0.004	0.64	*LOG*	*0.20*	*0.001*	*0.32*	LOG	0.19	0.002	0.54	(R720 - R729)/(R720 + R729 -2*R726)	P detection	(Wang et al., 2016a)
SR (R800, R635) PSSRb	L	0.16	0.005	0.64	*LOG*	*0.17*	*0.004*	*0.33*	LOG	0.15	0.006	0.55	R 800 / R 635	photosyntesis	(Blackburn, 1998)
NDVI (R544, R551)	L	0.16	0.005	0.64	*L*	*0.17*	*0.004*	*0.33*	L	0.16	0.005	0.55	(R544 - R551)/(R544 + R551)	P detection	(Kawamura et al., 2011)
OVI (R830, R660, R670) RDVI	L	0.12	0.018	0.66	*L*	*0.12*	*0.017*	*0.34*	L	0.09	0.035	0.57	((R830/R660) -1) / sqr((R830/R670) + 1)	vegetation presence	(Chen, 1996)
NDVI (R1080, R1460)	LOG	0.11	0.020	0.66	*LOG*	*0.09*	*0.043*	*0.34*	LOG	0.10	0.032	0.57	(R1080 - R1460) / (R1080 + 1460)	P detection	(Mahajan et al., 2014)
SR (R950, R660)	L	0.11	0.022	0.66	*L*	*0.11*	*0.020*	*0.34*	LOG	0.08	0.057	0.58	R950 / R 660	N detection	(Zhu et al., 2007a)
NDVI (R870, R1450)	LOG	0.10	0.025	0.66	*LOG*	*0.09*	*0.044*	*0.34*	LOG	0.07	0.063	0.58	(R870 - R1450)/(R870 + R1450)	P detection	(Pimstein et al., 2011)
SR (R830, R660) RVI	L	0.09	0.034	0.67	*L*	*0.09*	*0.034*	*0.34*	L	0.07	0.075	0.58	R830 / R660	red-edge	(Jordan, 1969)

(*continued on next page*)

Table A1 (*continued*)

VI	Canopy N:P				*Canopy N*				Canopy P				Equation	Developped for	References
	Model	r^2	*p-value*	RRMSEcv	*Model*	r^2	*p-value*	*RRMSEcv*	Model	r^2	*p-value*	RRMSEcv			
NDVI (R1050, R1100)	L	0.09	0.035	0.67	*L*	*0.18*	*0.003*	*0.32*	L	0.05	0.136	0.59	(R1050 -R1100) / (R1050 + R1100)	N detection	(Pacheco-Labrador et al., 2014)
SD (R533, R565)	L	0.08	0.045	0.67	*L*	*0.08*	*0.055*	*0.34*	L	0.07	0.066	0.58	R533 - R565	N detection	(Tian et al., 2011)
NDVI (R1645, R1715)	L	0.08	0.048	0.68	*L*	*0.07*	*0.068*	*0.34*	L	0.09	0.035	0.58	(R1645 - R1715)/(R1645 + R 1715)	P detection	(Pimstein et al., 2011)
NDVI (R1680, R1510) NDNI	LOG	0.07	0.075	0.68	*LOG*	*0.04*	*0.202*	*0.35*	LOG	0.07	0.064	0.58	(R1680 - R1510) / (R1680 + R1510)	N detection	(Serrano et al., 2002)
SR (R950, R680)	L	0.07	0.079	0.68	*L*	*0.07*	*0.079*	*0.34*	L	0.04	0.166	0.59	R950 / R 680	N detection	(Zhu et al., 2007a)
NDVI (R830, R660) NDVI	L	0.06	0.089	0.69	*L*	*0.06*	*0.086*	*0.35*	L	0.06	0.101	0.58	(R830 - R660)/(R830 + R660)	vegetation presence	(Huete and Jackson, 1987)
SR (R800, R680) PSSRa	L	0.05	0.111	0.69	*L*	*0.05*	*0.121*	*0.35*	L	0.04	0.202	0.59	R 800 / R680	photosyntesis	(Blackburn, 1998)
NDVI (R915, R920)	L	0.05	0.116	0.69	*L*	*0.07*	*0.076*	*0.35*	L	0.04	0.201	0.59	(R915 - R920) / (R915 + R920	N detection	(Pacheco-Labrador et al., 2014)
NDVI (R825, R1120)	L	0.04	0.189	0.69	*L*	*0.05*	*0.140*	*0.35*	L	0.01	0.573	0.60	(R825 - R1120) / (R825 + R1120)	N detection	(Pacheco-Labrador et al., 2014)
ND (R533, R565)	L	0.02	0.292	0.70	*L*	*0.03*	*0.222*	*0.36*	L	0.03	0.240	0.59	abs(R533 -R565)/(R533 + R565)	N detection	(Tian et al., 2011)
SR (R533, R565)	LOG	0.02	0.292	0.70	*LOG*	*0.03*	*0.222*	*0.36*	LOG	0.03	0.240	0.59	R533 / R565	N detection	(Tian et al., 2011)
SR (R890, R437)	LOG	0.02	0.352	0.70	*LOG*	*0.01*	*0.592*	*0.36*	L	0.01	0.418	0.60	(R890 / R437)	N detection	(Mirik et al., 2005)
NDVI (R653, R688)	L	0.01	0.496	0.70	*L*	*0.03*	*0.260*	*0.35*	L	0.01	0.449	0.61	(R653 - R688)/(R653 + R688)	P detection	(Kawamura et al., 2011)
NDVI (R531, R570) PRI	L	0.01	0.540	0.71	*L*	*0.01*	*0.444*	*0.36*	L	0.01	0.452	0.60	(R531 - R570) /(R531 + R570)	photosynthesis	(Gamon et al., 1997)
TBVI (R800, R445, R680) SIPI	L	0.00	0.713	0.71	*L*	*0.00*	*0.645*	*0.36*	L	0.00	0.699	0.60	(R800 -R445) / (R800 -R680)	chlorophyll	(Peñuelas et al., 1995)
SR (R1129, R462)	LOG	0.00	0.727	0.70	*LOG*	*0.01*	*0.470*	*0.36*	LOG	0.00	0.792	0.60	(1129 / R462)	P detection	(Mirik et al., 2005)
TBVI (R830, R660, R670) SAVI	LOG	0.00	0.739	0.72	*LOG*	*0.00*	*0.884*	*0.37*	LOG	0.00	0.854	0.60	1.5*(R830 - R660)/(R830 + R670 + 0.5)	vegetation presence	(Huete, 1988)
NDVI (R573, R540)	L	0.00	0.804	0.71	*L*	*0.00*	*0.994*	*0.36*	L	0.00	0.967	0.60	(R573 -R540) / (R573 + R540)	N detection	(Hansen and Schjoerring, 2003)
OVI (R830, R660) RDVI	LOG	0.00	0.828	0.72	*L*	*0.00*	*0.862*	*0.36*	LOG	0.00	0.934	0.60	(R830 -R 660) /sqr(R830 + R660)	photosynthesis	(Roujean and Breon, 1995)
NDVI (R662, R686)	L	0.00	0.829	0.70	*L*	*0.00*	*0.846*	*0.36*	L	0.00	0.645	0.61	(R662 - R686)/(R662 + R686)	P detection	(Kawamura et al., 2011)
NDVI (R523, R583)	L	0.00	0.857	0.71	*L*	*0.00*	*0.708*	*0.36*	L	0.00	0.670	0.60	(R523 - R583)/(R523 + R583)	P detection	(Kawamura et al., 2011)
OVI (R800, R670) OSAVI	L	0.00	0.890	0.72	*L*	*0.00*	*0.818*	*0.37*	L	0.00	0.872	0.60	(1 + 0.16) * (R800 - R670)/(R800 + R670 + 0.16)	vegetation presence	(Rondeaux et al., 1996)
SR (R800, R470) PSSRc	L	0.00	0.909	0.71	*L*	*0.00*	*0.673*	*0.36*	L	0.00	0.878	0.60	R800 / R 470	photosyntesis	(Blackburn, 1998)
NDVI (R1200, R1290)	L	0.00	0.999	0.70	*L*	*0.01*	*0.544*	*0.35*	L	0.00	0.706	0.60	(R1200 -R1290)/(R1200 + R1290)	N detection	(Pacheco-Labrador et al., 2014)

Table A2
Optimized vegetation indices for each canopy trait and each VI category (SR, SD, ND, TB1, TB2 and TB3). Bands composing the VI (λ1, λ2 and λ3, nm), coefficient of determination (r^2) and the Relative Root Mean Square error of cross validation (RRMSEcv) are showed. The results are showed for the original narrow band spectra and the spectra resampled to satellite sensors bands (MSI, aboard Sentinel 2, OLCI, aboard Sentinel 3, MODIS aboard Terra – Aqua, and OLI, aboard Landsat 8). SD = Simple difference; SR = Simple Ratio; ND = Normalized Difference, TB = Three Bands indices, PAN = Panchromatic band.

sensor	canopy trait	VI category	λ1 (nm)	λ2 (nm)	λ3 (nm)	r^2	*p-value*	RRMSEcv
narrow band sensor	Canopy N:P	SR	427	524		0.71	0.000	0.38
	Canopy N:P	SD	718	1577		0.59	0.000	0.45
	Canopy N:P	ND	427	524		0.70	0.000	0.39
	Canopy N:P	TB1	491	661	531	0.71	0.000	0.37
	Canopy N:P	TB2	531	411	541	0.70	0.000	0.38
	Canopy N:P	TB3	541	421	531	0.72	0.000	0.37
	Canopy N	SR	428	529		0.67	0.000	0.20
	Canopy N	SD	717	1833		0.58	0.000	0.23
	Canopy N	ND	428	529		0.66	0.000	0.21
	Canopy N	TB1	531	541	411	0.67	0.000	0.20
	Canopy N	TB2	531	411	551	0.67	0.000	0.20
	Canopy N	TB3	431	2431	561	0.69	0.000	0.20
	Canopy P	SR	422	524		0.66	0.000	0.36
	Canopy P	SD	717	1553		0.53	0.000	0.42
	Canopy P	ND	422	524		0.66	0.000	0.35
	Canopy P	TB1	531	541	421	0.67	0.000	0.35
	Canopy P	TB2	421	531	541	0.66	0.000	0.35
	Canopy P	TB3	721	521	451	0.64	0.000	0.36
MSI	Canopy N:P	SR	443	560		0.67	0.000	0.40
	Canopy N:P	SD	2190	705		0.53	0.000	0.48
	Canopy N:P	ND	443	560		0.67	0.000	0.40
	Canopy N:P	TB1	443	560	490	0.67	0.000	0.40
	Canopy N:P	TB2	560	443	490	0.66	0.000	0.41
	Canopy N:P	TB3	560	560	443	0.68	0.000	0.39
	Canopy N	SR	443	560		0.64	0.000	0.21
	Canopy N	SD	2190	705		0.55	0.000	0.24
	Canopy N	ND	443	560		0.63	0.000	0.22
	Canopy N	TB1	443	560	490	0.63	0.000	0.21
	Canopy N	TB2	705	490	2190	0.65	0.000	0.21
	Canopy N	TB3	2190	705	490	0.66	0.000	0.21
	Canopy P	SR	443	560		0.63	0.000	0.37
	Canopy P	SD	443	490		0.48	0.000	0.44
	Canopy P	ND	443	560		0.63	0.000	0.37
	Canopy P	TB1	443	560	490	0.64	0.000	0.36
	Canopy P	TB2	443	560	490	0.62	0.000	0.37
	Canopy P	TB3	705	560	443	0.62	0.000	0.37
OLCI	Canopy N:P	SR	412.5	560		0.67	0.000	0.40
	Canopy N:P	SD	490	510		0.50	0.000	0.50
	Canopy N:P	ND	412.5	560		0.67	0.000	0.40
	Canopy N:P	TB1	490	665	560	0.68	0.000	0.39
	Canopy N:P	TB2	560	442.5	400	0.67	0.000	0.40
	Canopy N:P	TB3	400	560	442.5	0.69	0.000	0.39
	Canopy N	SR	412.5	560		0.64	0.000	0.21
	Canopy N	SD	490	510		0.49	0.000	0.25
	Canopy N	ND	412.5	560		0.64	0.000	0.21
	Canopy N	TB1	490	620	560	0.64	0.000	0.21
	Canopy N	TB2	560	442.5	400	0.64	0.000	0.21
	Canopy N	TB3	400	560	442.5	0.66	0.000	0.21
	Canopy P	SR	490	510		0.63	0.000	0.37
	Canopy P	SD	490	510		0.49	0.000	0.44
	Canopy P	ND	490	510		0.63	0.000	0.37
	Canopy P	TB1	442.5	560	510	0.64	0.000	0.37
	Canopy P	TB2	510	490	412.5	0.64	0.000	0.36
	Canopy P	TB3	708.75	510	442.5	0.63	0.000	0.37
MODIS	Canopy N:P	SR	421.5	531		0.69	0.000	0.39
	Canopy N:P	SD	2130	555		0.50	0.000	0.50
	Canopy N:P	ND	421.5	531		0.68	0.000	0.39
	Canopy N:P	TB1	488	667	531	0.72	0.000	0.37
	Canopy N:P	TB2	531	412.5	421.5	0.70	0.000	0.38
	Canopy N:P	TB3	421.5	555	531	0.71	0.000	0.38
	Canopy N	SR	421.5	531		0.66	0.000	0.21
	Canopy N	SD	2130	555		0.54	0.000	0.24

(*continued on next page*)

Table A2 (*continued*)

sensor	canopy trait	VI category	λ1 (nm)	λ2 (nm)	λ3 (nm)	r^2	*p-value*	RRMSEcv
	Canopy N	ND	421.5	531		0.65	0.000	0.21
	Canopy N	TB1	488	645	531	0.66	0.000	0.21
	Canopy N	TB2	531	421.5	555	0.67	0.000	0.21
	Canopy N	TB3	421.5	555	531	0.67	0.000	0.20
	Canopy P	SR	421.5	531		0.63	0.000	0.37
	Canopy P	SD	443	531		0.48	0.000	0.44
	Canopy P	ND	421.5	531		0.64	0.000	0.36
	Canopy P	TB1	531	551	421.5	0.64	0.000	0.36
	Canopy P	TB2	421.5	531	555	0.65	0.000	0.36
	Canopy P	TB3	551	469	443	0.63	0.000	0.37
OLI	Canopy N:P	SR	443	562		0.68	0.000	0.40
	Canopy N:P	SD	443	590		0.48	0.000	0.50
	Canopy N:P	ND	482	590		0.67	0.000	0.40
	Canopy N:P	TB1	443	590	562	0.68	0.000	0.39
	Canopy N:P	TB2	590	482	443	0.67	0.000	0.40
	Canopy N:P	TB3	562	562	443	0.69	0.000	0.39
	Canopy N	SR	443	562		0.64	0.000	0.21
	Canopy N	SD	2200	562		0.51	0.000	0.25
	Canopy N	ND	443	562		0.63	0.000	0.22
	Canopy N	TB1	482	590	562	0.64	0.000	0.21
	Canopy N	TB2	562	482	2200	0.64	0.000	0.21
	Canopy N	TB3	2200	562	482	0.66	0.000	0.21
	Canopy P	SR	443	562		0.63	0.000	0.37
	Canopy P	SD	443	562		0.46	0.000	0.45
	Canopy P	ND	443	562		0.64	0.000	0.37
	Canopy P	TB1	443	562	482	0.64	0.000	0.37
	Canopy P	TB2	562	443	482	0.63	0.000	0.37
	Canopy P	TB3	562	562	443	0.62	0.000	0.38
WorldView 4	Canopy N:P	SR	480	545		0.63	0.000	0.42
	Canopy N:P	SD	480	545		0.48	0.000	0.51
	Canopy N:P	ND	480	545		0.63	0.000	0.42
	Canopy N:P	TB1	480	672	545	0.67	0.000	0.40
	Canopy N:P	TB2	545	480	PAN	0.55	0.000	0.47
	Canopy N:P	TB3	480	480	545	0.64	0.000	0.42
	Canopy N	SR	480	545		0.61	0.000	0.22
	Canopy N	SD	480	545		0.48	0.000	0.26
	Canopy N	ND	480	545		0.60	0.000	0.22
	Canopy N	TB1	545	545	480	0.60	0.000	0.22
	Canopy N	TB2	545	480	PAN	0.56	0.000	0.23
	Canopy N	TB3	PAN	545	480	0.64	0.000	0.21
	Canopy P	SR	545	480		0.60	0.000	0.38
	Canopy P	SD	480	545		0.46	0.000	0.45
	Canopy P	ND	480	545		0.59	0.000	0.38
	Canopy P	TB1	480	480	545	0.60	0.000	0.38
	Canopy P	TB2	480	545	PAN	0.54	0.000	0.41
	Canopy P	TB3	PAN	545	480	0.60	0.000	0.38
RapidEye	Canopy N:P	SR	475	555		0.64	0.000	0.42
	Canopy N:P	SD	475	555		0.48	0.000	0.51
	Canopy N:P	ND	475	555		0.65	0.000	0.42
	Canopy N:P	TB1	475	658	555	0.67	0.000	0.40
	Canopy N:P	TB2	555	475	710	0.59	0.000	0.45
	Canopy N:P	TB3	710	555	475	0.66	0.000	0.41
	Canopy N	SR	475	555		0.61	0.000	0.22
	Canopy N	SD	475	555		0.47	0.000	0.26
	Canopy N	ND	475	555		0.61	0.000	0.22
	Canopy N	TB1	555	555	475	0.61	0.000	0.22
	Canopy N	TB2	555	475	710	0.60	0.000	0.22
	Canopy N	TB3	710	555	475	0.65	0.000	0.21
	Canopy P	SR	555	475		0.61	0.000	0.38
	Canopy P	SD	475	555		0.46	0.000	0.45
	Canopy P	ND	475	555		0.60	0.000	0.38
	Canopy P	TB1	475	475	555	0.60	0.000	0.38
	Canopy P	TB2	555	475	710	0.57	0.000	0.40
	Canopy P	TB3	710	555	475	0.61	0.000	0.38

Table A3
Relationship between existing vegetation indices (VIs), calculated with the spectra resampled to satellite sensors of four satellites, with canopy N:P, canopy N and canopy P. The satellite sensors included MSI, aboard Sentinel 2, OLCI, aboard Sentinel 3, MODIS aboard Terra – Aqua, and OLI, aboard Landsat 8. No existing VI was calculated for the RapidEye and WorldView 4 sensors because their band positions are too distant (> 100 nm) from the nominal VIs' wavelengths. Coefficient of determination (r^2), p-value and Relative Root Mean Square Error of cross-validation ($RRMSE_{cv}$). The model between the variables is either linear (L) or logarithmic (LOG). The VIs were classified into four categories: ND = Normalized difference; SR = simple ratio; TB = Three band; OVI = other vegetation index.

Sensor	VI	Canopy N:P				Canopy N				Canopy P			
		Model	r^2	*p-value*	RRMSEcv	Model	r^2	*p-value*	RRMSEcv	Model	r^2	*p-value*	RRMSEcv
MSI	TB (R498, R413, R442)	LOG	0.62	0.000	0.43	LOG	0.58	0.000	0.23	LOG	0.62	0.000	0.38
	TB (R434, R496, R401)	L	0.63	0.000	0.43	L	0.58	0.000	0.23	L	0.62	0.000	0.38
	ND (R735, R1285)	L	0.30	0.000	0.58	L	0.29	0.000	0.30	L	0.21	0.001	0.53
	TB (R705, R717, R491)	LOG	0.41	0.000	0.54	LOG	0.35	0.000	0.29	L	0.35	0.000	0.48
	TB (R760, R705, R445)	L	0.31	0.000	0.58	L	0.31	0.000	0.29	LOG	0.32	0.000	0.50
	SR (R990, R720)	LOG	0.27	0.000	0.60	LOG	0.29	0.000	0.30	LOG	0.26	0.000	0.52
	OVI (R670, R700, R740, R780) REP	LOG	0.29	0.000	0.59	LOG	0.33	0.000	0.29	LOG	0.32	0.000	0.50
OLCI	TB (R498, R413, R442)	LOG	0.40	0.000	0.54	LOG	0.35	0.000	0.28	LOG	0.43	0.000	0.46
	TB (R434, R496, R401)	L	0.33	0.000	0.57	L	0.28	0.000	0.30	L	0.38	0.000	0.48
	TB (R705, R717, R491)	L	0.39	0.000	0.54	LOG	0.36	0.000	0.28	L	0.35	0.000	0.48
	TB (R760, R705, R445)	LOG	0.30	0.000	0.58	LOG	0.32	0.000	0.29	LOG	0.32	0.000	0.50
	SR (R990, R720)	LOG	0.30	0.000	0.59	LOG	0.32	0.000	0.29	LOG	0.28	0.000	0.51
	OVI (R670, R700, R740, R780) REP	L	0.29	0.000	0.59	L	0.32	0.000	0.29	L	0.32	0.000	0.50
MODIS	TB (R498, R413, R442)	LOG	0.36	0.000	0.56	LOG	0.31	0.000	0.29	LOG	0.40	0.000	0.47
	TB (R434, R496, R401)	L	0.36	0.000	0.55	L	0.31	0.000	0.29	L	0.40	0.000	0.47
	ND (R1220, R710)	L	0.07	0.063	0.68	L	0.07	0.068	0.34	L	0.05	0.144	0.59
	ND (R735, R1285)	L	0.23	0.001	0.61	L	0.25	0.000	0.31	L	0.14	0.008	0.55
	TB (R705, R717, R491)	LOG	0.02	0.286	0.70	LOG	0.02	0.327	0.36	LOG	0.02	0.392	0.60
	TB (R760, R705, R445)	L	0.08	0.050	0.68	L	0.06	0.101	0.35	L	0.06	0.089	0.58
	SR (R990, R720)	LOG	0.15	0.007	0.65	LOG	0.21	0.001	0.31	LOG	0.11	0.022	0.57
	OVI (R670, R700, R740, R780) REP	LOG	0.26	0.000	0.60	LOG	0.29	0.000	0.30	LOG	0.27	0.000	0.51
OLI	TB (R498, R413, R442)	LOG	0.55	0.000	0.47	LOG	0.50	0.000	0.25	LOG	0.55	0.000	0.41
	TB (R434, R496, R401)	L	0.55	0.000	0.47	L	0.50	0.000	0.25	L	0.55	0.000	0.41
	TB (R705, R717, R491)	LOG	0.27	0.000	0.60	LOG	0.21	0.001	0.32	LOG	0.19	0.002	0.54

References

Bakker, M.A., Carreño-Rocabado, G., Poorter, L., 2011. Leaf economics traits predict litter decomposition of tropical plants and differ among land use types. Funct. Ecol. 25, 473–483.

Blackburn, G.A., 1998. Spectral indices for estimating photosynthetic pigment concentrations: a test using senescent tree leaves. Int. J. Remote Sens. 19, 657–675.

Buschmann, C., Nagel, E., 1993. In vivo spectroscopy and internal optics of leaves as basis for remote sensing of vegetation. Int. J. Remote Sens. 14, 711–722.

Chen, J.M., 1996. Evaluation of vegetation indices and a modified simple ratio for boreal applications. Can. J. Remote. Sens. 22, 229–242.

Cho, M.A., Ramoelo, A., Debba, P., Mutanga, O., Mathieu, R., van Deventer, H., Ndlovu, N., 2013. Assessing the effects of subtropical forest fragmentation on leaf nitrogen distribution using remote sensing data. Landsc. Ecol. 28, 1479–1491.

Clevers, J.G.P.W., Gitelson, A.A., 2013. Remote estimation of crop and grass chlorophyll and nitrogen content using red-edge bands on sentinel-2 and-3. Int. J. Appl. Earth Obs. Geoinf. 23, 344–351.

Corp, L.A., Middleton, E.M., Campbell, P.K.E., Huemmrich, K.F., Daughtry, C.S.T., Russ, A.L., Cheng, Y.B., 2010. Spectral indices to monitor nitrogen-driven carbon uptake in field corn. J. Appl. Remote Sens. 4.

Dash, J., Curran, P.J., 2004. The MERIS terrestrial chlorophyll index. Int. J. Remote Sens. 25, 5403–5413.

Evans, J.R., 1989. Photosynthesis and nitrogen relationships in leaves of C3 plants. Oecologia 78, 9–19.

Ferwerda, J.G., Skidmore, A.K., Mutanga, O., 2005. Nitrogen detection with hyperspectral normalized ratio indices across multiple plant species. Int. J. Remote Sens. 26, 4083–4095.

Fitzgerald, G., Rodriguez, D., O'Leary, G., 2010. Measuring and predicting canopy nitrogen nutrition in wheat using a spectral index—the canopy chlorophyll content index (CCCI). Field Crops Res. 116, 318–324.

Fujita, Y., Venterink, H.O., Van Bodegom, P.M., Douma, J.C., Heil, G.W., Hölzel, N., Jabłońska, E., Kotowski, W., Okruszko, T., Pawlikowski, P., De Ruiter, P.C., Wassen, M.J., 2014. Low investment in sexual reproduction threatens plants adapted to phosphorus limitation. Nature 505, 82–86.

Gamon, J.A., Serrano, L., Surfus, J.S., 1997. The photochemical reflectance index: an optical indicator of photosynthetic radiation use efficiency across species, functional types, and nutrient levels. Oecologia 112, 492–501.

Gitelson, A.A., Kaufman, Y.J., Merzlyak, M.N., 1996. Use of a green channel in remote sensing of global vegetation from EOS- MODIS. Remote Sens. Environ. 58, 289–298.

Gitelson, A.A., Viña, A., Ciganda, V., Rundquist, D.C., Arkebauer, T.J., 2005. Remote estimation of canopy chlorophyll content in crops. Geophys. Res. Lett. 32, 1–4.

Gökkaya, K., Thomas, V., Noland, T., McCaughey, H., Morrison, I., Treitz, P., 2015. Mapping continuous forest type variation by means of correlating remotely sensed metrics to canopy N: P ratio in a boreal mixedwood forest. Appl. Veg. Sci. 18, 143–157.

Green, D.S., Erickson, J.E., Kruger, E.L., 2003. Foliar morphology and canopy nitrogen as predictors of light-use efficiency in terrestrial vegetation. Agric. For. Meteorol. 115, 163–171.

Güsewell, S., 2004. N:P ratios in terrestrial plants: variation and functional significance. New Phytol. 164, 243–266.

Güsewell, S., 2005. High nitrogen : phosphorus ratios reduce nutrient retention and second-year growth of wetland sedges. New Phytol. 166, 537–550.

Güsewell, S., Koerselman, W., Verhoeven, J.T.A., 2003. Biomass N:P ratios as indicators of nutrient limitation for plant populations in wetlands. Ecol. Appl. 13, 372–384.

Hansen, P.M., Schjoerring, J.K., 2003. Reflectance measurement of canopy biomass and nitrogen status in wheat crops using normalized difference vegetation indices and partial least squares regression. Remote Sens. Environ. 86, 542–553.

Homolová, L., Malenovský, Z., Clevers, J.G.P.W., García-Santos, G., Schaepman, M.E., 2013. Review of optical-based remote sensing for plant trait mapping. Ecol. Complex. 15, 1–16.

Horler, D.N.H., Dockray, M., Barber, J., 1983. The red edge of plant leaf reflectance. Int. J. Remote Sens. 4, 273–288.

Huete, A.R., 1988. A soil-adjusted vegetation index (SAVI). Remote Sens. Environ. 25, 295–309.

Huete, A.R., Jackson, R.D., 1987. Suitability of spectral indices for evaluating vegetation characteristics on arid rangelands. Remote Sens. Environ. 23, 213–IN218.

Jordan, C.F., 1969. Derivation of leaf-area index from quality of light on the forest floor. Ecology 50, 663–666.

Kawamura, K., Mackay, A.D., Tuohy, M.P., Betteridge, K., Sanches, I.D., Inoue, Y., 2011. Potential for spectral indices to remotely sense phosphorus and potassium content of legume-based pasture as a means of assessing soil phosphorus and potassium fertility status. Int. J. Remote Sens. 32, 103–124.

Kergoat, L., Lafont, S., Arneth, A., Le Dantec, V., Saugier, B., 2008. Nitrogen controls plant canopy light-use efficiency in temperate and boreal ecosystems. J. Geophys. Res. Biogeosci. 113.

Koerselman, W., Meuleman, A.F.M., 1996. The vegetation N:P ratio: a new tool to detect the nature of nutrient limitation. J. Appl. Ecol. 33, 1441–1450.

Kumar, L., Schmidt, K., Dury, S., Skidmore, A., 2006. Imaging spectrometry and vegetation science. In: Meer, F.D.v.d., Jong, S.M.D. (Eds.), Imaging Spectrometry: Basic Principles and Prospective Applications. Springer, Netherlands, Dordrecht, pp. 111–155.

le Maire, G., François, C., Soudani, K., Berveiller, D., Pontailler, J.-Y., Bréda, N., Genet, H., Davi, H., Dufrêne, E., 2008. Calibration and validation of hyperspectral indices for the estimation of broadleaved forest leaf chlorophyll content, leaf mass per area, leaf area index and leaf canopy biomass. Remote Sens. Environ. 112, 3846–3864.

Li, L.J., Zeng, D.H., Yu, Z.Y., Fan, Z.P., Mao, R., Peri, P.L., 2011. Foliar N/P ratio and nutrient limitation to vegetation growth on Keerqin sandy grassland of North-east

China. Grass Forage Sci. 66, 237–242.
Li, F., Miao, Y., Feng, G., Yuan, F., Yue, S., Gao, X., Liu, Y., Liu, B., Ustin, S.L., Chen, X., 2014. Improving estimation of summer maize nitrogen status with red edge-based spectral vegetation indices. Field Crops Res. 157, 111–123.
Loozen, Y., Rebel, K.T., Karssenberg, D., Wassen, M.J., Sardans, J., Peñuelas, J., De Jong, S.M., 2018. Remote sensing of canopy nitrogen at regional scale in Mediterranean forests using the spaceborne MERIS Terrestrial Chlorophyll Index. Biogeosciences 15, 2723–2742.
Mahajan, G.R., Sahoo, R.N., Pandey, R.N., Gupta, V.K., Kumar, D., 2014. Using hyperspectral remote sensing techniques to monitor nitrogen, phosphorus, sulphur and potassium in wheat (Triticum aestivum L.). Precis. Agric. 15, 499–522.
Mirik, M., Norland, J.E., Crabtree, R.L., Biondini, M.E., 2005. Hyperspectral one-meter-resolution remote sensing in Yellowstone National Park, Wyoming: I. Forage nutritional values. Rangel. Ecol. Manag. 58, 452–458.
Olde Venterink, H., Wassen, M.J., Verkroost, A.W.M., De Ruiter, P.C., 2003. Species richness-productivity patterns differ between N-, P-, and K-limited wetlands. Ecology 84, 2191–2199.
Pacheco-Labrador, J., González-Cascón, R., Pilar Martín, M., Riaño, D., 2014. Understanding the optical responses of leaf nitrogen in mediterranean holm oak (Quercus ilex) using field spectroscopy. Int. J. Appl. Earth Obs. Geoinf. 26, 105–118.
Peñuelas, J., Baret, F., Filella, I., 1995. Semi-empirical indices to assess carotenoids/chlorophyll a ratio from leaf spectral reflectance. Photosynthetica 31, 221–230.
Pimstein, A., Karnieli, A., Bansal, S.K., Bonfil, D.J., 2011. Exploring remotely sensed technologies for monitoring wheat potassium and phosphorus using field spectroscopy. Field Crops Res. 121, 125–135.
R Development Core Team, 2014. R: a Language and Environment for Statistical Computing, Computer Program. R Foundation for Statistical Computing, Vienna, Austria.
Ramoelo, A., Skidmore, A.K., Cho, M.A., Schlerf, M., Mathieu, R., Heitkönig, I.M.A., 2012. Regional estimation of savanna grass nitrogen using the red-edge band of the spaceborne rapideye sensor. Int. J. Appl. Earth Obs. Geoinf. 19, 151–162.
Ramoelo, A., Skidmore, A.K., Schlerf, M., Heitkönig, I.M.A., Mathieu, R., Cho, M.A., 2013. Savanna grass nitrogen to phosphorous ratio estimation using field spectroscopy and the potential for estimation with imaging spectroscopy. Int. J. Appl. Earth Obs. Geoinf. 23, 334–343.
Reich, P.B., 2012. Key canopy traits drive forest productivity. Proceedings of the Royal Society B: Biological Sciences 279, 2128–2134.
Reich, P.B., Ellsworth, D.S., Walters, M.B., Vose, J.M., Gresham, C., Volin, J.C., Bowman, W.D., 1999. Generality of leaf trait relationships: a test across six biomes. Ecology 80, 1955–1969.
Roeling, I.S., Ozinga, W.A., van Dijk, J., Eppinga, M.B., Wassen, M.J., 2018. Plant species occurrence patterns in Eurasian grasslands reflect adaptation to nutrient ratios. Oecologia 186, 1055–1067.
Rondeaux, G., Steven, M., Baret, F., 1996. Optimization of soil-adjusted vegetation indices. Remote Sens. Environ. 55, 95–107.
Roujean, J.-L., Breon, F.-M., 1995. Estimating PAR absorbed by vegetation from bidirectional reflectance measurements. Remote Sens. Environ. 51, 375–384.
Schlemmer, M., Gitelson, A., Schepers, J., Ferguson, R., Peng, Y., Shanahan, J., Rundquist, D., 2013. Remote estimation of nitrogen and chlorophyll contents in maize at leaf and canopy levels. Int. J. Appl. Earth Obs. Geoinf. 25, 47–54.
Serrano, L., Peñuelas, J., Ustin, S.L., 2002. Remote sensing of nitrogen and lignin in Mediterranean vegetation from AVIRIS data: decomposing biochemical from structural signals. Remote Sens. Environ. 81, 355–364.
Sims, D.A., Gamon, J.A., 2002. Relationships between leaf pigment content and spectral reflectance across a wide range of species, leaf structures and developmental stages. Remote Sens. Environ. 81, 337–354.
Tessier, J.T., Raynal, D.J., 2003. Use of nitrogen to phosphorus ratios in plant tissue as an indicator of nutrient limitation and nitrogen saturation. J. Appl. Ecol. 40, 523–534.
Thenkabail, P.S., Smith, R.B., De Pauw, E., 2002. Evaluation of narrowband and broadband vegetation indices for determining optimal hyperspectral wavebands for agricultural crop characterization. Photogramm. Eng. Remote Sensing 68, 607–621.
Tian, Y.C., Yao, X., Yang, J., Cao, W.X., Hannaway, D.B., Zhu, Y., 2011. Assessing newly developed and published vegetation indices for estimating rice leaf nitrogen concentration with ground- and space-based hyperspectral reflectance. Field Crops Res. 120, 299–310.
Walker, A.P., Beckerman, A.P., Gu, L., Kattge, J., Cernusak, L.A., Domingues, T.F., Scales, J.C., Wohlfahrt, G., Wullschleger, S.D., Woodward, F.I., 2014. The relationship of leaf photosynthetic traits – vcmax and Jmax – to leaf nitrogen, leaf phosphorus, and specific leaf area: a meta-analysis and modeling study. Ecol. Evol. 4, 3218–3235.
Wang, W., Yao, X., Yao, X., Tian, Y., Liu, X., Ni, J., Cao, W., Zhu, Y., 2012. Estimating leaf nitrogen concentration with three-band vegetation indices in rice and wheat. Field Crops Res. 129, 90–98.
Wang, J., Wang, T., Skidmore, A.K., Shi, T., Wu, G., 2015. Evaluating different methods for grass nutrient estimation from canopy hyperspectral reflectance. Remote Sens. (Basel) 7, 5901–5917.
Wang, J., Shi, T., Liu, H., Wu, G., 2016a. Successive projections algorithm-based three-band vegetation index for foliar phosphorus estimation. Ecol. Indic. 67, 12–20.
Wang, Z., Wang, T., Darvishzadeh, R., Skidmore, A.K., Jones, S., Suarez, L., Woodgate, W., Heiden, U., Heurich, M., Hearne, J., 2016b. Vegetation indices for mapping canopy foliar nitrogen in a mixed temperate forest. Remote Sens. (Basel) 8, 491. https://doi.org/10.3390/rs8060491.
Wassen, M.J., Venterink, H.O.G.M., de Swart, E.O.A.M., 1995. Nutrient concentrations in mire vegetation as a measure of nutrient limitation in mire ecosystems. J. Veg. Sci. 6, 5–16.
Wassen, M.J., Venterink, H.O., Lapshina, E.D., Tanneberger, F., 2005. Endangered plants persist under phosphorus limitation. Nature 437, 547–550.
Wassen, M.J., de Boer, H.J., Fleischer, K., Rebel, K.T., Dekker, S.C., 2013. Vegetation-mediated feedback in water, carbon, nitrogen and phosphorus cycles. Landsc. Ecol. 28, 599–614.
Wright, I.J., Reich, P.B., Westoby, M., Ackerly, D.D., Baruch, Z., Bongers, F., Cavender-Bares, J., Chapin, T., Cornelissen, J.H.C., Diemer, M., Flexas, J., Garnier, E., Groom, P.K., Gulias, J., Hikosaka, K., Lamont, B.B., Lee, T., Lee, W., Lusk, C., Midgley, J.J., Navas, M.-L., Niinemets, U., Oleksyn, J., Osada, N., Poorter, H., Poot, P., Prior, L., Pyankov, V.I., Roumet, C., Thomas, S.C., Tjoelker, M.G., Veneklaas, E.J., Villar, R., 2004. The worldwide leaf economics spectrum. Nature 428, 821–827.
Xue, L., Cao, W., Luo, W., Dai, T., Zhu, Y., 2004. Monitoring leaf nitrogen status in rice with canopy spectral reflectance. Agron. J. 96, 135–142.
Yao, X., Zhu, Y., Tian, Y., Feng, W., Cao, W., 2010. Exploring hyperspectral bands and estimation indices for leaf nitrogen accumulation in wheat. Int. J. Appl. Earth Obs. Geoinf. 12, 89–100.
Zarco-Tejada, P.J., Berjón, A., López-Lozano, R., Miller, J.R., Martín, P., Cachorro, V., González, M.R., De Frutos, A., 2005. Assessing vineyard condition with hyperspectral indices: leaf and canopy reflectance simulation in a row-structured discontinuous canopy. Remote Sens. Environ. 99, 271–287.
Zhao, Q., Zeng, D.H., 2009. Diagnosis methods of N and P limitation to tree growth: a review. Chin. J. Ecol. 28, 122–128.
Zhu, Y., Tian, Y., Yao, X., Liu, X., Cao, W., 2007a. Analysis of common canopy reflectance spectra for indicating leaf nitrogen concentrations in wheat and rice. Plant Prod. Sci. 10, 400–411.
Zhu, Y., Zhou, D., Yao, X., Tian, Y., Cao, W., 2007b. Quantitative relationships of leaf nitrogen status to canopy spectral reflectance in rice. Aust. J. Agric. Res. 58, 1077–1085.